Analytical solutions of variable cross-section longitudinal porous fin with power exponents of thermal parameters

Pranab Kanti Roy[1], Bipattaran Raj[2, 3]
[1]*Department of Mechanical Engineering, Seacom Skills University, Kendradangal, Birbhum-731236, West Bengal, India*
[2]*Department of Mathematics, Seacom Skills University, Kendradangal, Birbhum-731236, West Bengal, India,*
[3]*Department of Mathematics, Chandidas Mahavidyalaya, Birbhum-731215, West Bengal, India*

Abstract- The present works find the analysis of longitudinal porous fins under the influence of an external magnetic field with multiple power law-dependent parameters. The rectangular cross-section of the porous fin is the base profile and four reduced profiles such as bigger edge (BE), conventional (Conv.), smaller edge (SE) and triangular are obtained by successive reduction of tip thickness. The five geometrical shapes of rectangular, BE, Conv., SE, and triangular profiles are described by variable crossectional area which in turn defined by profile index 0, ¼, ½, 3/4, and 1 of extended length and results in one non-singular and four different singular value equations. The energy equation of basic longitudinal fins is a non-singular equation, and all reduced longitudinal porous fins are dissimilar singular-type equations. The non-singular energy equations of longitudinal fins are solved by classical operator and four reduced longitudinal porous fins such as BE, Conv., SE, and triangular longitudinal porous fins are solved by the separate modified differential operator. The results obtained from classical ADM) are validated with the finite difference method (FDM) for the particular case of a basic rectangular porous fin. The parametric studies of various profiles on the temperature distribution are analyzed and presented.

Keywords: variable area; porosity; magnetic effect; modified differential operator

Nomenclature

k Thermal conductivity, W/mK

$T(x)$ Temperature function of fin length, K

P Perimeter at location x, m

T_b Dimensional temperature at the base, K

T_a Temperature at ambient condition, K

$q(T)$ Internal heat generation power function of (T, T_a, T_b), W/m^3

$h(T)$ Heat transfer co-efficient, W/m^2K

A, B, ε_G, z Power exponent

R_a Modified form of Rayleigh number, $\dfrac{gK\beta(T_b - T_a)L}{\alpha\gamma k_R\psi}$,

R_d Radiation-conduction parameter, $\dfrac{4\sigma T_a^{\,3}}{3k_{eff}\beta_R}$

R_2 Surface ambient-radiation parameter, $R_2 = \dfrac{4\sigma\varepsilon_s T_a^{\,3}L}{k_{eff}\psi}$

H Hartmann number, $\dfrac{\sigma_m B_0^{\,2}V^2L^2}{k_{eff}(T_b - T_a)}$

Z_0 Fin parameter, $\sqrt{h_bL^2/k_{eff}t_b}$

G Heat generation number, $\dfrac{q_0L^2}{k_{eff}(T_b - T_a)}$

k_R Thermal conductivity ratio, $\dfrac{k_{eff}}{k_f}$

k_{eff} Effective thermal conductivity, $k_s(1-\phi+\phi k_R)$, W/mK

x axial co-ordinate measured from fin tip , m

y vertical co-ordinate measured from fin tip, m

$A(x)$ Cross-section at the location x, m^2

X Dimensionless co-ordinate measured from fin tip, $\frac{x}{L}$,

J_c Conduction current density, A/m

E External electric field

B_0 Magnetic Field, $Tesla$

V_w Darchy velocity, m/s

V Macroscopic velocity of fluid due to electric and magnetic field, m/s

C_p Specific Heat, $J/kg-K$

b Width, m

t_b Thickness at the base, m

E Electrical field, V/m

$\varepsilon(T)$ Surface emissivity of power function of (T, T_a, T_b),

ϕ Parameter denote porosity

θ Temperature in dimensionless form, $\frac{T-T_a}{T_b-T_a}$

ε_s Emissivity parameter of surface w.r.t. atmosphere

σ Constant of Stephen-Boltzmann, W/m^2K^4

γ Kinematic viscosity, m^2/s

α Thermal diffusivity, $\frac{k_f}{\rho C_p}$

ρ Fluid density, kg/m^3

β Thermal expansion co-efficient, $1/K$

σ_m Electrical conductivity, A/m

β_R Mean absorption co-efficient of Rossland

ψ Aspect ratio, $\frac{t_b}{L}$

Subscripts

eff	effective properties
s	solid
f	fluid
a	ambient
b	base

1. INTRODUCTION

The extended surfaces are used for heat transfer enhancement have a remarkable application, for example, electronics engineering, automobile engineering, aerospace application and much more [1,2]. For the essential evolution of very powerful and reduced mass for maximum energy dissipating characteristics, porous extended surface provide practical and quick solution. The earlier research works was concentrated on the different operating parameters on the thermal feedback of porous surfaces in order to establish such anticipated application [3,4]. Kiwan, and Al-Nimr [5] presented between porous and solid surface of equal size with certain porosity parameter with different design and operating conditions. Subba Raddy and Bakier [6] investigated radiative porous fin by applying Darcy model and Rossland approximation for different boundary conditions. The mechanism of increasing heat transfer rate is to increase the effective surface area, which is made by interconnected voids that increases the convective-radiative heat dissipation from the surface. Gorla and Bakier [7] studied longitudinal rectangular porous fin in with combine mode of both convection and radiation in which Darchy's model is used for interaction between solid and fluid interaction. They proved mathematically that porous fins have better heat transfer characteristics as compared to solid fin. Kundu and Bhanja [8] presented the performance and optimization of longitudinal porous fin with different mathematical model.

For solving the problems of extended surface, literature is rich in many techniques to treat the non-linearity or linearity of the problem. Earlier researcher used perturbation theory [9] for finding the approximate solution of non-linear fin equation with the assumption of weak non-linearity and initial guess. In order to eliminate the problem of weak non-linearity, researcher amalgamated both theory perturbation methods with homotopy principle [10]. Saedodin and Shahbabaei [11] analyzed longitudinal

porous with homotopy perturbation method (HPM). Hatami et al [12] analyses porous fin of different materials with the help of differential transform method [DTM], collocation method [CM], least square method [LSM]. Oguntala et. al [13] applied Daftardar-Gejiji and Jafari Method (DJM) for the analysis of rectangular porous fin and the analytical results is also validated by fourth order Runge-kutta method. Liao [14] introduces the concept of embedded parameter for artificially controlling the convergence of non-linearity parameter in Homotopy analysis method (HAM). Fahd Abdelmouiz Ziari et al.[15] investgated the energy equation of fin by applying shooting technique while tips considering both insulated as well as convective boundary conditions and evaluted absolute error at the tips shows a good accuracy of results. Perez & Gonzalez [16] analysed computationally thermal-hydraulic performance of wavy fins having one, two, three or four rows of tubes and their the differences in the behavior from row to row are analyzed

Earlier works on longitudinal fins, researchers used mixed up mode power and linear law for their analysis. Roy et al.[17],Yasong Sun[18], Mohsen Torabi[19] studied longitudinal porous fin with multiple non-linearities with combination of linear and power law for the variation of thermophysical parameters. The recent research on the porous medium reveals that the applied electric and magnetic field on the nanoparticles with hybrid character shows a betterment of heat transfer rate than cavity flows [20]. Magnetic effects are also influence the micro-organism behavior study of bio-heat transfer as well as nanoparticle flow [21].

The porous fin with series of small holes so that magnetic field forces the ionized charged particles in the passage which increases the velocity as well as the heat transfer rate. The appreciable number of research works on porous fin with magnetic effect is done by M. G. Sobamowo [22]. They explained with the principle Lorenz force, the magnetic parameter has significant importance on the thermal performance of porous fin. Das and Kundu [23] presented the forward and inverse heat transfer analyses of porous fin under the combine application of magnetic field.

2. MATHEMATICAL ANALYSIS

Consider porous fin of rectangular section with dimension as a parent geometry as shown in Figure 1. It can be assumed that each cross-section of the porous fin can be obtained from its immediate larger geometry successively. As for example the bigger edge (BE) convex fin can be obtained from rectangular shape by suitable machining process and conventional (Conv.) convex profile can be obtained from previous BE convex profile. Likewise smaller edge (SE) can be obtained from Conv. convex fin and at last triangular shape from SE convex can be obtained by suitable manufacturing technique. All the five profile are subjected to constant electric and magnetic field with a internal heat generation. The steady flow energy equation for differential volume is as follows

$$q_x - q_{x+dx} + q(T)A(x)(1-\phi)dx = h(T)Pdx(T-T_a)(1-\phi) + \dot{m}C_p(T-T_a) + Pdx\sigma\varepsilon(T)\left(T^4 - T_a^4\right) + \phi\frac{J_c \times J_c}{\sigma_m}dx \quad (1)$$

Where the area of cross-sectional of the porous fin changes according to

$$A(x) = Wt(x) = Wt_b\left(\frac{x}{L}\right)^z \quad (2)$$

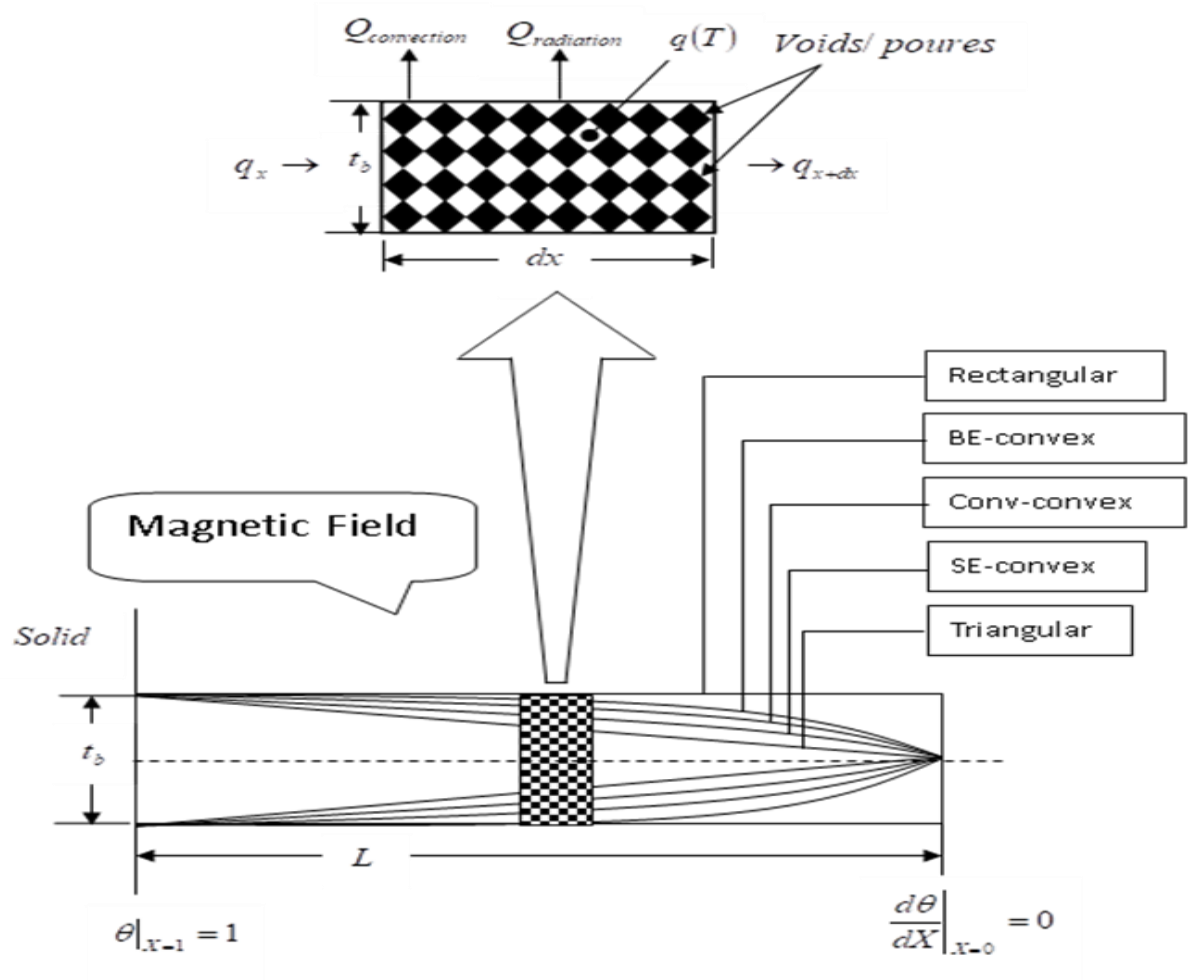

Figure 1. Schematic diagram of different cross-section of porous fin under uniform magnetic field

Where z is the profile index of non-dimensional length and its value can be in the range 0 to 1. For z=0 it corresponds to rectangular profile. If z increases from 0 to ¼, the tip thickness reduces and it corresponds to BE convex profile. For z= ½ the tip thicknes converted to the conventional (Conv.) convex profile and for z= ¾ it corresponds to SE edge, and for z=1, it is reduced to triangular convex porous fin respectively.

The heat transfer co-efficient is governed by power law [24]

$$h(T) = h_b \left(\frac{T - T_a}{T_b - T_a} \right)^A \tag{3a}$$

The same variations is applied for surface emissivity and heat generations

$$\varepsilon(T) = \varepsilon_s \left(\frac{T - T_a}{T_b - T_a} \right)^B \tag{3b}$$

$$q(T) = q_b \left(\frac{T - T_a}{T_b - T_a} \right)^{\varepsilon_G} \tag{3c}$$

The cross product of current density and their variations with area and velocity and temperature are related as follows

$$\frac{J_c \times J_c}{\sigma_m} = \sigma_m B_0{}^2 V^2 A(x)\left(\frac{T-T_a}{T_b-T_a}\right) \tag{4}$$

The fluid flows through the interconnected voids due to buoyancy effect and that is governed by Darcy's Law [25]. The heat transfer rate from the base of the fin is conduction combined with radiation and energy Eq. (1) can be as follows,

$$\frac{d}{dx}\left[X^z \frac{dT}{dx} + \frac{4\sigma}{3\beta_R k_{eff}} X^z \frac{dT^4}{dx}\right] + \frac{q_b}{k_{eff}}\left(\frac{T-T_a}{T_b-T_a}\right)^{\varepsilon_G} X^z(1-\phi) = \frac{h_b P}{W t_b k_{eff}}\left(\frac{T-T_a}{T_b-T_a}\right)^A (1-\phi)(T-T_a) +$$

$$\frac{\rho g K \beta C_p P(T-T_a)^2}{k_{eff} W t_b \gamma} + \frac{\sigma P \varepsilon_s T_a{}^3 \left(T^4 - T_a{}^4\right)}{k_{eff} W t_b}\left(\frac{T-T_a}{T_b-T_a}\right)^B + \frac{\phi \sigma_m B_0{}^2 u^2}{k_{eff} W t_b} W t_b X^z \left(\frac{T-T_a}{T_b-T_a}\right) \tag{5}$$

with the following boundary condition

$$at\ \ the\ \ tip\ \ x=0,\ \ \frac{dT}{dx}=0 \tag{6a}$$

$$at\ \ the\ \ base\ \ x=L,\ \ T=T_b \tag{6b}$$

using $T^4 \approx 4T_a{}^3 T - 3T_a{}^4$ and $width\ \ (W) \approx Perimeter\ \ (P)$ and employing the non dimensional terms, the energy Eq.(5) can be as follows,

$$\frac{d}{dX}\left[X^z \frac{d\theta}{dX} + \frac{16\sigma T_a{}^3}{3\beta_R k_{eff}} X^z \frac{d\theta}{dX}\right] + \frac{q_b L^2 (1-\phi)}{k_{eff}(T_b-T_a)} X^z \theta^{\varepsilon_G} = \frac{h_b L^2 (1-\phi)}{t_b k_{eff}} \theta^{A+1} + \frac{\rho g K \beta C_p L^2 (T_b-T_a)}{k_{eff} t_b \gamma} \theta^2 +$$

$$\frac{4\sigma \varepsilon_s T_a{}^3 L^2}{k_{eff} t_b} \theta^{B+1} + \frac{\phi \sigma_m B_0{}^2 u^2 L^2}{k_{eff}(T_b-T_a)} X^z \theta \tag{7}$$

The energy Eq(7) can be in dimensional less form as below

$$\frac{d}{dX}\left[X^z \frac{d\theta}{dX}\right] = -\frac{G(1-\phi)}{(1+4R_d)} X^z \theta^{\varepsilon_G} + \frac{Z_0{}^2 (1-\phi)}{(1+4R_d)} \theta^{A+1} + \frac{R_a}{\psi^2 (1+4R_d)} \theta^2 + \frac{R_2}{\psi^2 (1+4R_d)} \theta^{B+1}$$

$$+ \frac{\phi H_a}{(1+4R_d)} \theta \tag{8}$$

With the boundary condition

$$\left.\frac{d\theta}{dX}\right|_{X=0} = 0 \tag{9a}$$

$$\theta|_{X=1} = 1 \tag{9b}$$

4. APPLICATION OF CLASSICAL AND MODIFIED ADM

The Eq. [8] even though it is a non-linear but it can be either singular or non singular depending on the value profile index z. The principle of decomposition method introduced first time by Adomian G [26] and the theory has provision to solve separately the non-singular and singular value problem by classical Adomian decomposition method (ADM) and modified Adomian decomposition method (MADM) respectively in conjunction with the non-linearity effect. Both the theory spitted the given equation into linear and non-linear parts and the highest order derivative present in the equation is expressed as linear operator as in case of classical ADM and highest order derivative combining remainder term will form as modified differential operator in case of modified

MADM. The MADM has a wide flexibility of solving different types of singular value equations and each equation are expressed by different modified operator corresponding to the equations in order to solve that particular singular value equations. The advantages of both method are that operator of the method are not required to be discreatised, the linearization of non-linear terms are not required, the theory does not require the perturbation concept and solution converges rapidly.The linear and non-linear terms are decomposed by Adomian polynomials [27,28] and inverse operator is subsequently used to solve the resulting equations. Therefore the equation in operator form,

$$\frac{d^2\theta}{dX^2}+\frac{z}{X}\frac{d\theta}{dX}=-\frac{G(1-\phi)}{(1+4R_d)}\theta^{\varepsilon_G}+\frac{{Z_0}^2(1-\phi)}{(1+4R_d)}\left[\frac{\theta^{n+1}}{X^z}\right]+\frac{R_a}{\psi^2(1+R_d)}\left[\frac{\theta^2}{X^z}\right]+\frac{R_2}{\psi^2(1+4R_d)}\left[\frac{\theta^{B+1}}{X^z}\right]+$$

$$\frac{\phi H_a}{(1+4R_d)}\left[\frac{\theta}{X^z}\right] \quad for\ z=0,\frac{1}{4},\frac{1}{2},\frac{3}{4},1 \tag{10}$$

The generalized forward differential operator for the above equation can be written as

$$L_z(\bullet)=X^{-z}\frac{d}{dX}X^z\frac{d}{dX}(\bullet) \quad for\ z=0,\frac{1}{4},\frac{1}{2},\frac{3}{4},1\ .$$

The generalized forward differential operator, L_z is invertible, and there exist inverse operator ${L_z}^{-1}$ and it can be expressed as below,

$${L_z}^{-1}(\bullet)=\int_0^X X^{-z}\int_0^X X^z(\bullet)\,dXdX \quad for\ z=0,\frac{1}{4},\frac{1}{2},\frac{3}{4},1$$

By putting z=0, governing Eq. [10] is converted to non-singular and non-linear type equations, which is the case of rectangular profile. As the value of m changes to ¼, 1/2, ¾ and 1 respectively the energy equation[10] inturn converted to different singular value equations with same nonlinearity corresponding to BE, Conv., SE and triangular porous fin. The change of profile index of the length of logitudinal porous fins with corresponding variations of tip thickness are given in Table 1. Since all the equations contains common non-linearity and therefore non-linear terms are expanded in Adomians Polynomials.

Multiplying by inverse operator ${L_z}^{-1}$ on both side of the Eq. [10]

$${L_z}^{-1}L_z\theta=-\frac{G(1-\phi)}{(1+4R_d)}\left[{L_z}^{-1}\sum_0^\alpha A_\xi\right]+\frac{{Z_0}^2(1-\phi)}{(1+4R_d)}\left[{L_z}^{-1}\sum_0^\alpha\left(\frac{B_\xi}{X^z}\right)\right]+\frac{R_a}{\psi^2(1+4R_d)}\left[{L_z}^{-1}\sum\left(\frac{C_\xi}{X^z}\right)\right]+$$

$$\frac{R_2}{\psi^2(1+4R_d)}\left[{L_z}^{-1}\sum_0^\alpha\left(\frac{D_\xi}{X^z}\right)\right]+\frac{\phi H_a}{(1+4R_d)}\left[{L_z}^{-1}\sum_0^\alpha\left(\frac{E_\xi}{X^z}\right)\right] \quad for\ z=0,\frac{1}{4},\frac{1}{2},\frac{3}{4},1 \tag{11}$$

where non-linear terms are expended in terms of Adomian polynomials

$$NA=\theta^{\varepsilon_G}=\sum_{\xi=0}^{\alpha}A_\xi=[A_0;A_1;A_3;\cdots]=\left[{\theta_0}^{1-\varepsilon_G};(1-\varepsilon_G){\theta_0}^{-\varepsilon_G}\theta_1;(1-\varepsilon_G){\theta_0}^{-\varepsilon_G}\theta_2-\frac{\varepsilon_G(1-\varepsilon_G){\theta_0}^{-\varepsilon_G-1}{\theta_1}^2}{2};\cdots\right]$$

$$NB=\theta^{A+1}=\sum_{\xi=0}^{\alpha}B_\xi=[B_0;B_1;B_3;\cdots]=\left[{\theta_0}^{A+1};(A+1){\theta_0}^A\theta_1;(A+1){\theta_0}^A\theta_2+\frac{A(A+1){\theta_1}^2{\theta_0}^{A-1}}{2};\cdots\right]$$

$$NC=\theta^2=\sum_{\xi=0}^{\alpha}C_\xi=[C_0;C_1;C_3;\cdots]=\left[{\theta_0}^2;2\theta_0\theta_1;2\theta_0\theta_2+{\theta_1}^2;\cdots\right]$$

$$ND=\theta^{B+1}=\sum_{\xi=0}^{\alpha}D_\xi=[D_0;D_1;D_3;\cdots]=\left[{\theta_0}^{B+1};(B+1){\theta_0}^B\theta_1;(B+1){\theta_0}^B\theta_2+\frac{B(B+1){\theta_1}^2{\theta_0}^{B-1}}{2};\cdots\right]$$

And linear terms are expended as follows

$$NE = \theta = \sum_{\xi=0}^{\alpha} E_{\xi} = [E_0; E_1; E_3; \cdots] = [\theta_0; \theta_1; \theta_2; \cdots]$$

The above equation [11] is expanded according to Maclaurin series

$$L_z^{-1} L_z \theta = \theta_0 - \frac{G(1-\phi)}{(1+4R_d)}\left[L_z^{-1}\sum_0^{\xi} A_{\xi}\right] + \frac{Z_0{}^2(1-\phi)}{(1+4R_d)}\left[L_z^{-1}\sum_0^{\alpha}\left(\frac{B_{\xi}}{X^z}\right)\right] + \frac{R_a}{\psi^2(1+4R_d)}\left[L_z^{-1}\sum_0^{\alpha}\left(\frac{C_{\xi}}{X^z}\right)\right] +$$

$$\frac{R_2}{\psi^2(1+4R_d)}\left[L_z^{-1}\sum_0^{\alpha}\left(\frac{D_{\xi}}{X^z}\right)\right] + \frac{\phi H_a}{(1+4R_d)}\left[L_z^{-1}\sum_0^{\alpha}\left(\frac{E_{\xi}}{X^z}\right)\right] \quad for\ z = 0, \frac{1}{4}, \frac{1}{2}, \frac{3}{4}, 1 \qquad (12)$$

where $\theta_0 = \theta(0) + X\frac{d\theta(0)}{dX}$ is assumed to be a constant it is calculated in different manner for different profile as follows

$\theta_0 = \theta(0) + X\frac{d\theta(0)}{dX} = C + 0 \Rightarrow$ Rectangular porous fin

$\theta_0 = \theta(0) + X\frac{d\theta(0)}{dX} = C + 0 \Rightarrow$ BE-convex porous fin

$\theta_0 = \theta(0) + X\frac{d\theta(0)}{dX} = C + 0 \Rightarrow$ Conv. convex porous fin

$\theta_0 = \theta(0) + X\frac{d\theta(0)}{dX} = C \Rightarrow$ SE convex porous fin

$\theta_0 = \theta(0) + X\frac{d\theta(0)}{dX} = C \Rightarrow$ Triangular porous fin

The higher order terms for rectangular, BE-convex, Conv. Convex, SE-convex and triangular porous fin are calculated by the relation

$$\theta_{\xi+1} = -\frac{G(1-\phi)}{(1+4R_d)} L_m^{-1}\left(\sum_0^{\xi} A_{\xi}\right) + \frac{Z_0{}^2(1-\phi)}{(1+4R_d)} L_z^{-1}\left(\sum_0^{\alpha} B_{\xi}\right) + \frac{R_a}{\psi^2(1+4R_d)} L_z^{-1}\left(\sum_0^{\alpha} C_{\xi}\right) +$$

$$\frac{R_2}{\psi^2(1+4R_d)} L_z^{-1}\left(\sum_0^{\alpha} D_{\xi}\right) + \frac{\phi H_a}{(1+4R_d)} L_z^{-1}\left(\sum_0^{\alpha} E_{\xi}\right); \quad \xi \geq 0\ and\ z = 0, \frac{1}{4}, \frac{1}{2}, \frac{3}{4}, 1 \qquad (13)$$

After finding each component of temperature field separately for each profile, the final temperature field is obtained by the relation

$$\theta = \theta_0 + \theta_1 + \theta_2 + \cdots\cdots \qquad (14)$$

5. RESULTS AND DISCUSSION

The theories of decomposition method have been applied to solve the variable cross-sectional longitudinal porous fin while taking into consideration of magnetic field and power exponent of thermal parameters. There are five enengy equations corresponding to different cross-sections of longitudinal

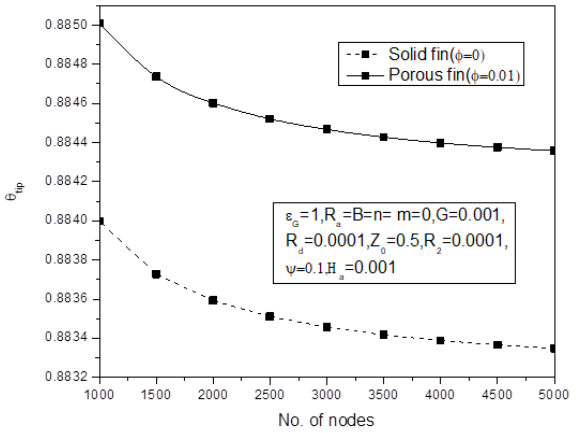

Figure 2. Tip temperature function of number of discreating grid points in FDM for solid and porous fin

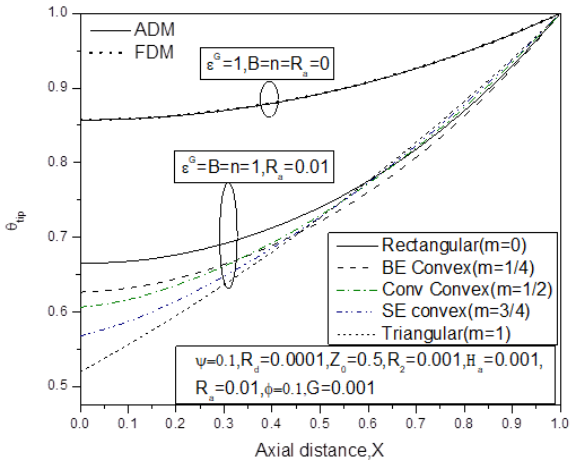

Figure 3. Temperature distribution of rectangular, BE, Conv. convex, SE and triangular porous fin along the axial length and comparison of ADM with FDM in special case of rectangular porous fin.

porous fin. One non singular type equations originated from rectangular porous fin and four different singular value singular value equations originated from different cross-sections of longitudinal porous fins. The one non-singular and four different singular value equations are solved by forward and inverse differential operator as explained in Table 1. Since increasing value of profile index of non dimensional length describe the successive reduction in thickness and it can be assumed that all the lighter profiles can be produced from the rectangular shape and for validation of decomposition results, only case of rectangular (z=0) porous fin is considered in which numerical scheme, finite difference method (FDM) has been adopted for comparison. The equation is linearised by putting $\varepsilon_G = 1, n = 0, Ra = 0$ *and* $B = 0$ and the equation is discreatised with unknown grid points (N) and the central difference scheme is has been used for interior nodes and backward difference from tip ends. The selection of grid for the present analysis is up to 5000 nodes. The large value of thermo-physical parameters leads to a high non-linearity in the solution which ultimately increases the absolute error at the tip. The lager values of absolute error at the tip leads to an unreliable results of the method. Although, addition of more number of terms may improve the solution of the series but it requires heavy computational work and memory requirement. Therefore present analyses consider upto 4th terms of the decomposition series and 5000 nodes of numerical method. The ranges of parameter selected for the present analysis are $G = 0.1 - 0.001$,

$\varepsilon_G = B = n = \frac{1}{2} - \frac{1}{2}\ 2,\ \phi = 0 - 0.95,$

$R_a = 0 - 0.01,\ R_d = 0 - 0.0001,$

$\phi = 0 - 0.95,\ \psi = 0.1 - 0.5,\ H_a = 0 - 0.001.$

The numerical code is executed is executed at different grid points ranging from 1000

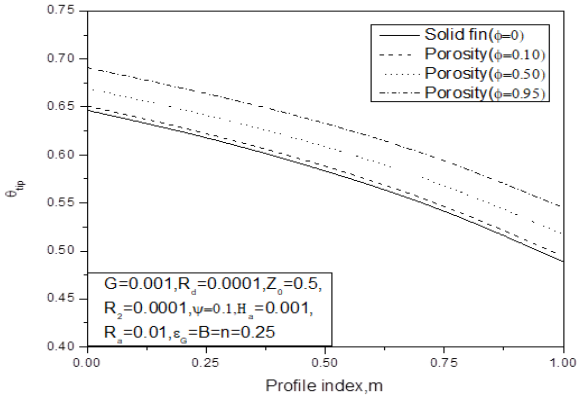

Figure 4. Effect of tip temperature of various profiles with respect to profile index for different values of porosity values.

to 5000 separately for the case of solid and porous fin as shown in Figure 2. The temperature distribution obtained from both of the decomposition methods are demonstrated in Figure 3. It is found that shape of temperature distribution curves obtained from rectangular, BE convex, Conv. convex, SE convex and triangular porous are different. The temperature distribution curve of triangular profile from tip to base is linear in nature and it is lowest among all the profiles. The temperature distribution of rectangular fin is non-linear in nature its value highest among all the profile. The results of classical decomposition methods and numerical results of FDM are compared are compared in special case when $\varepsilon_G = 1, B = n = R_a = 0$. It has been observed both the FDM and ADM are good agreement in the special case of rectangular porous fin. The Figure 4 shows the variation of tip temperature with respect to the profile index, m. The LHS of the horizontal co-ordinate indicates i.e. when m=0 represents the

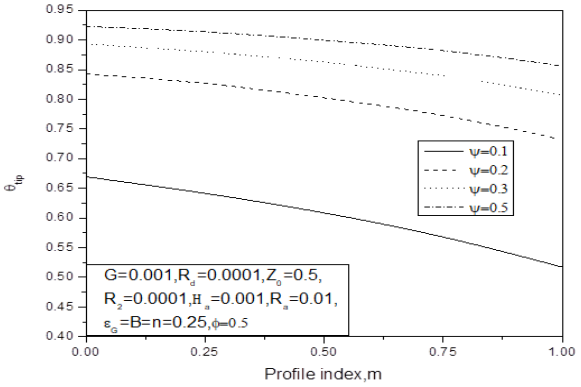

Figure 5. Effect of tip temperature of various profiles with respect to profile index for different values of aspect ratio.

rectangular profile and RHS of co-ordinates represents the triangular profile and vertical co-ordinates represent tip temperature of all intermediate profile. The intermediate vertical co-ordinates represent corresponding to points 0, 25, 0.50 and 0.75 are the temperature of BE-convex, Con. Convex and SE-convex profile respectively. As the profile changes from rectangular to triangular, the tip shape decreases progressively that results fins of lighter structure and tip temperature has a decreasing trends of temperature as the profile of the porous fin changes from rectangular to triangular . The bottom curve represents the temperature of solid fin and all the curves above it represent the temperature of porous fin at different values of porosity values along the profile index. The relative spacing between the lines are constant which indicates that porosity parameter is independent of profile index. Physically porosity of

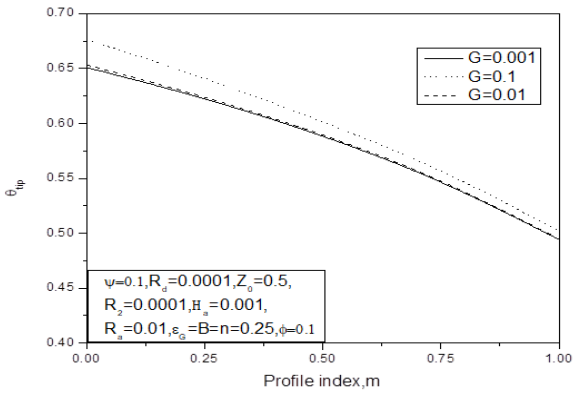

Figure 6. Effect of tip temperature of various profiles with respect to profile index for different values of heat generation number.

any porous medium indicates the creation of empty spaces in the solid that reduces the thermal conductivity of solid due to removal of solid materials and increases the effective surface area. The reduction of thermal conductivity in the solid reduces the heat transfer in the solid matrix as well as heat generation and simultaneously increases the effective surface area for increasing the heat transfer by convection and radiation from the solid surface. Higher value of porosity results more empty space and better convection and radiation and the higher is the temperature than the solid fin.

Figure 5 illustrate the variation tip temperature with respect to the profile index m at different values of aspect ratio. The aspect ratio is a parameter that gives the relationship between length and thickness of

porous fin and it is practically important for design and thermal aspect point of view. The tip temperature is lower for lower value of aspect ratio and it is higher for higher aspect ratio for all the

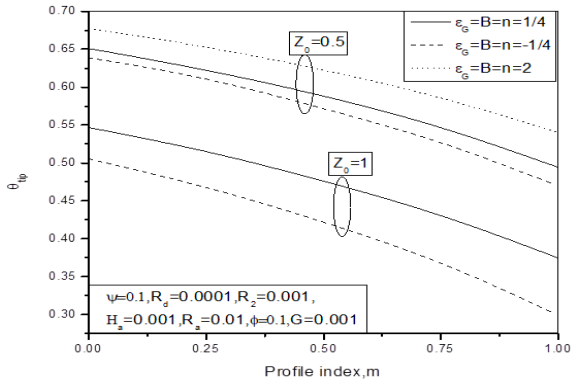

Figure 7. Effect of tip temperature of various profiles with respect to profile index for different values of heat transfer co-efficient.

profiles. But the relative spacing between the temperature lines is diverging trends as profile of the porous fin changes from rectangular to triangular shape.

Figure 6 explain the variation of tip temperature with respect to the profile index, m for different values of . The heat generation is highest in case of rectangular profile and decreases progressively as profile index m changes to ¾, 1/2, 1/4 and it is lowest for triangular profile at different values of heat generation number. In general, tip temperature is higher at higher values of heat generation and it is lower at lower values of heat generation. It is evident from the figure that the relative spacing between the tip

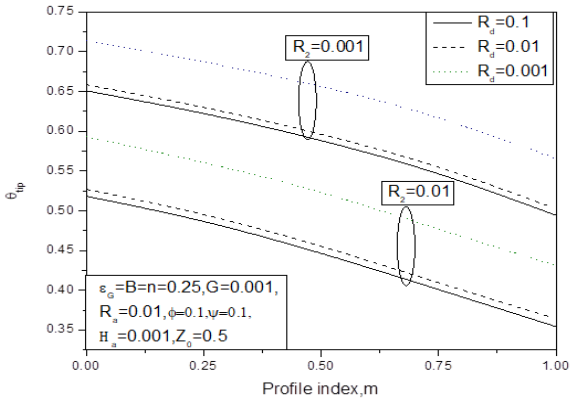

Figure 8. Effect of tip temperature of various profiles with respect to profile index for different values of Radiation conduction parameter.

temperature lines is more in rectangular profile than the triangular profile. It is due to the fact since the heat generation is with respect to solid materials only therefore the heavier materials has higher tip temperature than the lighter profile.

Figure 7 shows the variation of tip temperature with respect to m for different values of ε_G. The specific values of ε_G 0.25, -0.25 and 2 corresponds to laminar natural convection, laminar film boiling and nucleate boiling respectively. The tip temperature is higher for the value of Z_0=0.5 and it has lower value for Z_0=1 for all values of ε_G. Tip temperature is higher for rectangular profile and as the profile index changes from rectangular to triangular, the tip temperature has decreasing trends and it has lowest value for triangular profile. The relative spacing between the tip temperatures corresponding to different values of ε_G has a diverging trend at higher value of Z_0.

Table 1 Formation of classical and modified differential operator different type fins

ADM

Geometry	Classical forward operator	Classical inverse operator
Rectangular	$L_0 = \frac{d^2}{dX^2}(\bullet)$	$L_0^{-1}(\bullet) = \int_0^X \int_0^X (\bullet) dX dX$
MADM Modified inverse operators		Modified forward operators
BE-Convex	$L_{\frac{1}{4}} = X^{-\frac{1}{4}} \frac{d}{dX} X^{\frac{1}{4}} \frac{d}{dX}(\bullet)$	$L_{\frac{1}{4}}^{-1}(\bullet) = \int_0^X X^{-\frac{1}{4}} \int_0^X X^{\frac{1}{4}} (\bullet) dX dX$
Conventional Convex	$L_{\frac{1}{2}} = X^{-\frac{1}{2}} \frac{d}{dX} X^{\frac{1}{2}} \frac{d}{dX}(\bullet)$	$L_{\frac{1}{2}}^{-1}(\bullet) = \int_0^X X^{-\frac{1}{2}} \int_0^X X^{\frac{1}{2}} (\bullet) dX dX$
SE-Convex	$L_{\frac{3}{4}} = X^{-\frac{3}{4}} \frac{d}{dX} X^{\frac{3}{4}} \frac{d}{dX}(\bullet)$	$L_{\frac{3}{4}}^{-1}(\bullet) = \int_0^X X^{-\frac{3}{4}} \int_0^X X^{\frac{3}{4}} (\bullet) dX dX$
Triangular	$L_1 = X^{-1} \frac{d}{dX} X \frac{d}{dX}(\bullet)$	$L_1^{-1}(\bullet) = \int_0^X X^{-1} \int_0^X X (\bullet) dX dX$

Figure 8 show the variation of tip temperature with respect to m at two values of R_2 0.01 and 0.001 respectively. For each value of R_2, the values of R_d are taken 0.1, 0.01 and 0.001 respectively. It has been found that the tip temperature is higher for lower value of R_2 and R_d and all the tip temperature lines are decreasing trends and constant spacing from rectangular to triangular profiles, i.e. the profile index has no impact on the tip temperature.

6. CONCLUSIONS

An analytical solution of longitudinal porous fin with variable cross-sections with power law dependent of co-efficient of heat transfer, surface emissivity and heat generation are analyzed. The rectangular, BE, Conv. convex, convex, SE and triangular porous fin are obtained by changing the profile index 0, 1/4, 1/2, 3/4 and 1 respectively. One non-singular equation corresponding to rectangular profile is solved by classical operator described by classical Adomian decomposition method (ADM) theory and four different singular value equations with same nonlinearity are solved by different modified operators as described by modified Adomian decomposition method (MADM) theory. The results obtained from classical ADM are validated with the finite difference method (FDM) for the special case of rectangular porous fin. The effects of various thermo-physical parameters on the temperature distribution are presented.

REFERENCES

[1] Kem D.Q, Kraus D.A. (1972). Extended Surface Heat Transfer. McGraw–Hill, New York.

[2] Kim, S. Y., Paek, J. W., and Kang, B. H. 2000. "Flow and Heat Transfer Correlations for Porous Fin in a Plate-Fin Heat Exchanger," Journal of Heat Transfer: 122 (3): 572–578. DOI: https://doi.org/10.1115/1.1287170.

[3] Vaszi, A. Z., Elliott, L., Ingham, D. B., and Pop, I. 2004. "Conjugate Free Convection from vertical Plate Fin with a Rounded Tip Embedded in a Porous Medium," International Journal of Heat and Mass Transfer: 47(12–13): 2785–2794. DOI: https://doi.org/10.1080/716100521.

[4] Kiwan, S., and Zeitoun, O. 2008. "Natural Convection in a Horizontal Cylindrical Annulus Using Porous Fins", International Journal of Numerical Methods for Heat and Fluid Flow: 18(5): 618–634. DOI: http://dx.doi.org/10.1108/09615530810879747.

[5] Kiwan, S., and Al-Nimr, M. A. 2001. "Using Porous Fins for Heat Transfer Enhancement," Journal of Heat Transfer: 123(4): 790–795. DOI: https://doi.org/10.1115/1.1371922.

[6] Rama Subba Reddy Gorla and A.Y. Bakier. 2011. "Thermal Analysis of natural convection and radiation in porous fin" International Communication in Heat and Mass Transfer 38: 638-645. DOI: https://doi.org/10.1016/j.icheatmasstransfer.2010.12.024.

[7] Rama Gorla A.Y. Bakier, "Thermal analysis of natural convection and radiation in porous fins, International Communications in Heat and Mass Transfer,2007, 38(5):638-645

[8] Balaram Kundu, Dipankar Bhanja, An analytical prediction for performance and optimum design analysis of porous fins", International Journal of Refrigeration,2011, 34 :337-352.

[9] Martínez-Carranza, J., Soto-Eguibar, F. & Moya-Cessa, H. 2012. "Alternative analysis to perturbation theory in quantum mechanics." *The European Physical Journal D*: 66(22): DOI: https://doi.org/10.1140/epjd/e2011-20654-5.

[10] J. H. He. 1999. "Homotopy perturbation technique" Computer Methods in Applied Mechanics and Engineering: 178(3-4): 257-262. DOI: https://doi.org/10.1016/S0045-7825(99)00018-3.

[11] Saedodin, S., Shahbabaei. M. 2013. "Thermal Analysis of Natural Convection in Porous Fins with Homotopy Perturbation Method (HPM)". Arabian Journal for Science and Engineering: 38:2227–2231. DOI: https://doi.org/10.1007/s13369-013-0581-6.

[12] M. HatamiA. Hasanpour D.D.Ganji. 2013. "Heat transfer study through porous fins (Si_3N_4 and AL) with temperature-dependent heat generation" Energy conversion and Management: 74(9-16). DOI: https://doi.org/10.1016/j.enconman.2013.04.034.

[13] Oguntala, G., Sobamowo, G., Abd-Alhameed, Stephen Jones. 2019. "Efficient Iterative Method for Investigation of Convective–Radiative Porous Fin with Internal Heat Generation under a Uniform Magnetic Field" *Int. J. Appl. Comput. Math* :5(13): DOI: https://doi.org/10.1007/s40819-018-0592-9.

[12] Turkyilmazoglu, M. 2014."Efficiency of Heat and MassTransfer in FullyWet Porous Fins: Exponential Fins versus Straight Fins" International

Journal of Refrigeration: 46:158–164: DOI: https://doi.org/10.1016/j.ijrefrig.2014.04.011.
[14] S.J. Liao. 1992. "The proposed homotopy analysis technique for the solution of nonlinear problems" Ph.D. Thesis, Shanghai Jiao Tong University.
[15] Fahd Abdelmouiz ziar, Achour Benslama., & Khaled Ferkous. 2023. A shooting method solution for a convective-radiative straight longitudinal fin with variable thermal properties and nonlinear boundary conditions "International Journal of Energy for a Clean Environment" 24(3) 2023:63-81: DOI: 10.1615/InterJEnerCleanEnv.2022041661.
[16] Ruben B. Perez & Juan J. Gonzalez. 2023. Heat transfer and pressure drop Mechanisms in wavy fins having one, Two, three, and four rows of tubes "International Journal of Energy for a Clean Environment 19(1–2):49–65 (2018): DOI: 10.1615/InterJEnerCleanEnv.2018021015.
[17] Pranab Kanti Roy, Ashis Mallick, Hiranmoy Mondal, Sicelo Goqo, Precious Sibanda. 2017. "Numerical study on rectangular-convex-triangular profiles with all variable thermal properties" International Journal of Mechanical Sciences: 133:251-259. DOI: https://doi.org/10.1016/j.ijmecsci.2017.07.066.
[18] Ya-song Sun, Jin-Liang Xu. 2015. "Thermal performance of continuously moving radiative-convective fin of complex cross-section with multiple non-linearities" International Communications in Heat and Mass Transfer: 63: 23-34. DOI: https://doi.org/10.1016/j.icheatmasstransfer.2015.01.011.
[19] Mohsen Torabi, Abdul Aziz, Kaili Zhang. 2013. "A comparative study of longitudinal fins of rectangular, trapezoidal and concave parabolic profiles with multiples non linierities" Energy: 51:243-256. DOI: https://doi.org/10.1016/j.energy.2012.11.052.
[20] Hosseinzadeh, K., Roghani, S., Mogharrebi, A. R., Asadi, A., and Ganji, D. D. 2021 "Optimization of Hybrid Nanoparticles with Mixture Fluid Flow in an Octagonal Porous Medium by Effect of Radiation and Magnetic Field," Journal of Thermal Analysis and Calorimetry: 143:1413–1424. DOI: https://doi.org/10.1007/s10973-020-10376-9.
[21] Hosseinzadeh, K., Salehi, S., Mardani, M. R., Mahmoudi, F. Y.,Waqas, M., and Ganji, D. D. 2020. "Investigation of Nano-Bioconvective Fluid Motile Microorganism and Nanoparticle Flow by Considering MHD and Thermal Radiation," Informatics in Medicine Unlocked: 21: 100462. https://doi.org/10.1016/j.imu.2020.100462.
[22] M. G. Sobamowo, K.C. Alaribe, A.O. Adeleye. 2020 "A Study on the Impact of Lorentz Force on the Thermal Behaviour of a Convective-Radiative Porous Fin using Differential Transformation Method" International Journal of Mechanical Dynamics & Analysis: 6:45-58:
[23] Das R, B. Kundu. 2012. "Predicting of heat generation and electromagnetic parameters from temperature response in porous fin" Journal of Thermo-physics and heat transfer: 6:45-58. DOI: https://doi.org/10.2514/1.T6224.
[24] S.P.Law, R.H. Yeh. 1994. "Fins with temperature dependent surface heat flux-I: single heat transfer mode "Int. Journal of Heat and Mass Transfer: 37:1509-1512. DOI: https://doi.org/10.1016/0017-9310(94)90152-X.
[25] L.Preziosi A.Farina. 2002."On Darcy's law for growing porous media" International Journal of Non-Linear Mechanics :37 (3): 485-491. DOI: https://doi.org/10.1016/S0020-7462(01)00022-1.
[26] Adomian G. 1994. Solving frontier problems in physics: the decomposition method. Dordrecht: Kluwer Academic Publishers.
[27] Roy Pranab Kanti, A decomposition solution of variable thickness absorber plate solar collectors with power law dependent thermal conductivity, ASME-J. Therm. Sci. Eng. Appl. 14 (8) (2022), 084501.
[28] Bhowmik A, Singla RK, Roy Pranab K, Prasad DK, Das R, Repaka R. 2013. " Predicting geometry of rectangular and hyperbolic fin profiles with temperature-dependent thermal properties using decomposition and evolutionary methods" Energy Convers Manage 2013: 74:535–547. DOI: https://doi.org/10.1016/j.enconman.2013.07.025.